NRIAG Journal of Astronomy and Geophysics 6 (2017) 230–243

Contents lists available at ScienceDirect

NRIAG Journal of Astronomy and Geophysics

journal homepage: www.elsevier.com/locate/nrjag

Full length article

Evaluation of groundwater potentiality survey in south Ataqa-northwestern part of Gulf of Suez by using resistivity data and site-selection modeling

Sultan Awad Sultan [a], Khalid Sayed Ahmed Tawfik Essa [b], Mohamed Hassan Khalil [b], Alaa Eldin Hassan El-Nahry [c], Alaa Nayef Hasan Galal [c,*]

[a] National Research Institute of Astronomy and Geophysics, Helwan, Egypt
[b] Geophysics Department, Faculty of Science, Cairo University, Egypt
[c] National Authority for Remote Sensing and Space Sciences, Egypt

ARTICLE INFO

Article history:
Received 4 December 2016
Accepted 17 February 2017
Available online 17 March 2017

ABSTRACT

The integration between advanced techniques for groundwater exploration is necessary to manage and protect the vital resources. Direct current (DC) resistivity geoelectrical technique, Enhanced Thematic Mapper Landsat (ETM+) images and a geographic information system (GIS) are integrated to identify the groundwater potentiality in the study area. The interpretation of the one-dimensional (1-D) inversion of the acquired resistivity data are implemented for mapping the fresh to slightly brackish water aquifer. This number of vertical electric sounding is quite enough for different geologic mapping. The depth to the top of the ground water table (obtained from the existing Water well) and subsurface lithological information are used to calibrate the results of the resistivity data inversion. This research discussed how the integration between the geoelectrical parameters and hydrological data, could be used to determine the appropriate locations of dams construction and recommend the appropriate methods for management and rehabilitation of the aquifer.

1. Introduction

1.1. Overview

The north western part of Gulf of Suez region is considered as one of the important investment area in Egypt. It considers the national industrial project area that known as "DEVELOPMENT OF NORTH PART OF EASTERN DEREST" that is very important source of the national income of Egypt canal. The study area is located in the north western part of Gulf of Suez region between latitudes 29°46′N and 29°48′N and longitudes 32°16′E and 32°20′E (Fig. 1). It is bordered by Gulf of Suez from east, Gebel Ataqa from North, Wadi Badaa from south and some heights such as Gebel EL-Kahalyia and Gebel Abu Trifya from west. It comprises the new harbor of North El-Sukhna at the Gulf of Suez and the newly developed industrial zone as well. The study area received water from the rainfall or flash flood. It may be mitigated by storing water available during rainy periods for human and agricultural needs (Fig. 1). It had seen potential growth in connection with development projects, new urbanization, oil exploration, land reclamation, and tourism. It is likely that such growth will expand in the future and may even serve as a base for further commercial, industrial, and agricultural development activities. Large-scale economic growth of south Ataqa will certainly attract a large number of people from the presently overcrowded population centers in the country. Consequently, this growth will significantly increase the demand for fresh water in the area.

In this research, systematic planning and managing for groundwater exploration using modern techniques is implemented for the proper utilization, protection and management of this vital resource. Direct current (DC) resistivity geoelectrical method, Enhanced Thematic Mapper Landsat (ETM+) image, geographic information system (GIS) are integrated to achieve this approach.

* Corresponding author.
E-mail address: alaa_nayef@hotmail.com (A.N.H. Galal).

Peer review under responsibility of National Research Institute of Astronomy and Geophysics.

Production and hosting by Elsevier

http://dx.doi.org/10.1016/j.nrjag.2017.02.002

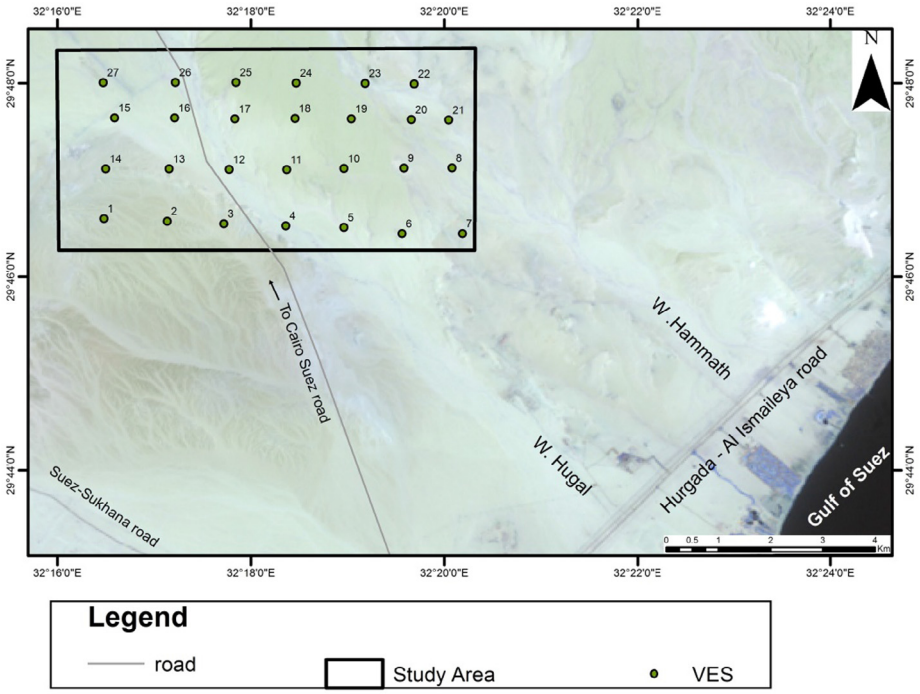

Fig. 1. Location satellite image of the study area.

Remotely sensed data are used to delineate the alluvial active channels, which were integrated with morphometric parameters extracted from digital elevation models (DEM) into geographical information systems (GIS) to construct a hydrological model that provided stream orders of each basin to decide the suitable solution in determining locations of dams.

A direct current (DC) resistivity geoelectric technique is applied on south Ataqa area to determine and evaluate the main aquifer in this area. The well-known Schlumberger configuration (VES) of electrode separation ranging from AB/2 = 1.5 m to AB/2 = 1000 m is used for measuring the twenty-seven VES stations.

Extensive work was been carried out to retrieve the groundwater quality in the densely populated and/or highly developed areas such as south Ataqa. A number of previous geological, hydrological, and geophysical studies were carried out in south Ataqa by many researchers (Sadek, 1926; Butzer, 1960; Abdallah and Abd El-Hady, 1966; Youssef et al., 1966; Ettinger and Langozki, 1969; Youssef and Abd Rahman, 1978; Abd El Nasr, 1979; Renolds, 1979; Teufik, 1988; Moustafa and Abdallah, 1991; Abdallah and Alindani, 1993; Abu El-Enain et al., 1995; Sultan and Mohamed, 2000; Abd El Rahman, 2001; Abu El-Anwar and El-Gohary, 2003; El Attar,2003; Masoud and Koike, 2005; Khalil, 2006; Hassan, 2008; Mills and Shata, 2009; Sultan et al., 2015)

2. Geological setting

2.1. Surface geology

In the study area, different rock units were identified. They range in age from the Jurassic to Quaternary. Eocene, Oligocene and Miocene are the most widespread rock units in this area (Hassan, 2008) (Fig. 2). The Jurassic section consists of varicolored and cross-bedded sandstones, with mudstone and siltstone interbeds. The Cretaceous succession in the study area is classified by into three rock units, which are (from base to top) the Malha, Galala and chalky limestone units. The Eocene rocks are the nummulitic limestones. It form the main part of Gabal Ataqa and Gabal El-Galala El-Bahariya as well as the Faulted blocks of Akheider-Rammlyia and Um Zeita-Kahallya. The Eocene succession is subdivided from base to top into the upper part of Esna Shale Formation, Farafra Formation, Thebes Formation, Muweilih Formation, Mokattam Formation, Observatory Formation, Qurn Formation, Wadi Garawi Formation and Wadi Hof Formation. The Oligocene rocks are differentiated into two units; the lower unit is varicolored, consisting of unstratified sands, gravels, and sedimentary quartzites; the upper unit crops out in the central part of the study area and consists of basalt sheets of Gabal El Ahmer Formation. The Miocene succession that is exposed in the Sadat area lies 30 km to the southwest of Suez city and is subdivided from base to top as follows: Sadat Formation (Early Miocene), Hommath Formation (Middle Miocene) and Hagul Formation (Late Miocene). Sands, gravels, clays, sabkhas and sand accumulations represent the recent deposits in the study area.

The Lithostratigraphy of the Eocene exposures in the north Eastern Desert has been a subject of study for many authors. The most important are those carried out by Cuvillier (1941), Al Ahwani, 1982, Strougo (1985a, 1985b), Strougo and Boukhary, 1987, Abd-Elshafy et al. (1989), Strougo and Abdallah, 1990, Abu El-Enain et al., 1995, Bignot and Strougo (2002).

2.2. Structural setting

The study area is a depression situated between El Galala El Bahariya plateau and Gebel Ataqa tablelands, which is highly deformed. The depression represents a horsted block of considerable extent and magnitude (Norconsult, 1979). Generally, faulting primarily controls the depression and its adjacent localities. However, the folding and unconformity are noticeable in several sites. The structural pattern in the study area plays an important role in the aquifers hydraulic connection. In the area under study, the most pronounced structural elements are represented by the following (Fig. 2).

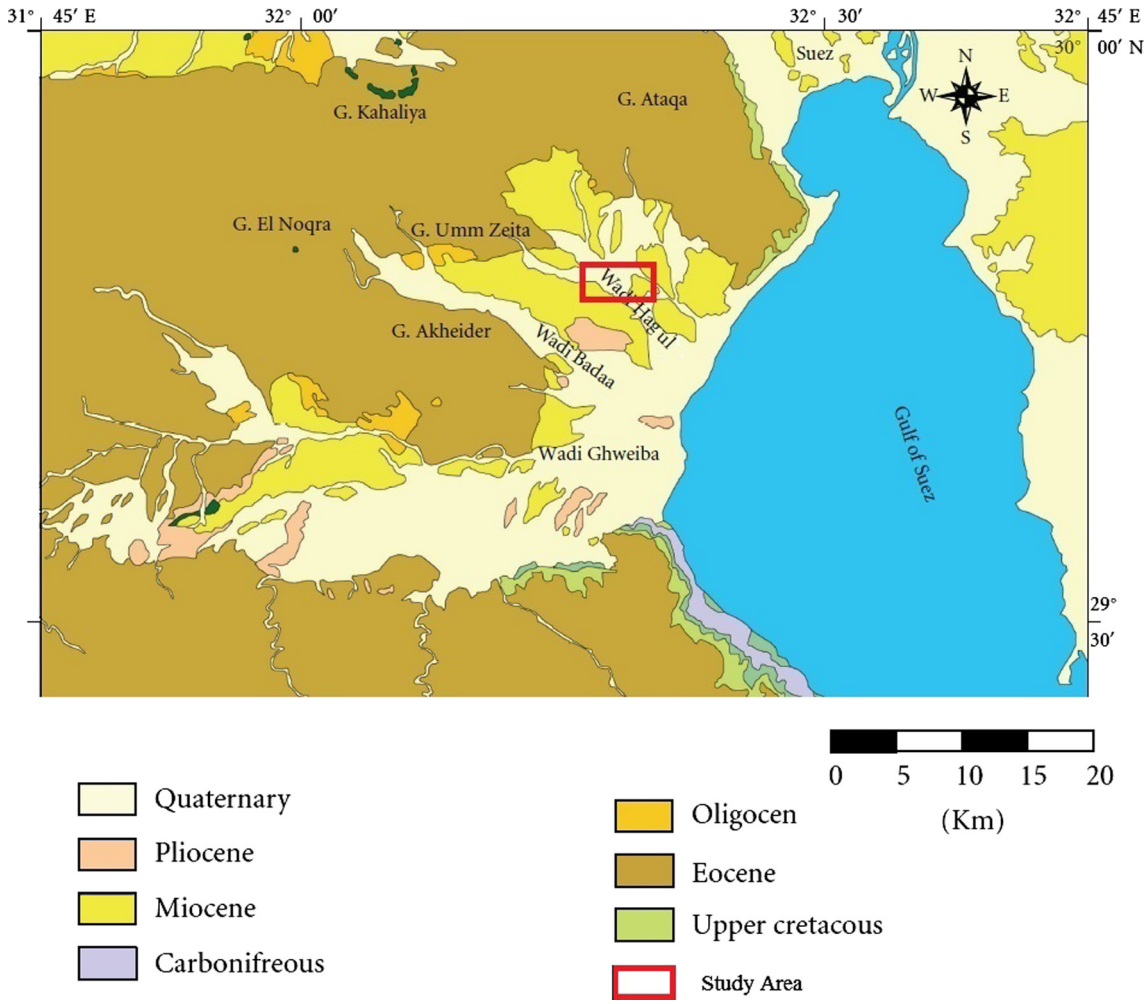

Fig. 2. Geologic map of the study area (compiled after CONOCO).

2.3. The faults

The area between Gebel Ataqa and the Northern Galala Plateau is considered to be the junction between two main provinces; the Gulf of Suez to the east and the Cairo Suez district to the north and northwest. The faults comprise the following.

2.3.1. NNW-SSE faults

The Northwestern-Southeastern faults are the majority in number, which have relatively small angle of dip, large throws and moderate throw length ratios. The faults belonging to this set are dominant and are mainly of gravity type. They bound the major wadis of the study area (e.g. Wadi Hammtih, Wadi Hagul, Wadi Badaa and Wadi Ghoweiba) and affect the Eocene limestone plateau.

2.3.2. E-W faults

The East-West faults generally have high angles of dip, moderate lengths, large throws and moderate throw length ratios. The faults of this set are second in importance. The E-W faulting however is believed to be started in the late Eocene and continued during the Oligocene (Salem, 1988).

2.3.3. WNW-ESE faults

The WNW faults have high angles of dip, short lengths, small throws and small throw length ratios. The set of faults is distributed in the low hilly area in the depression between Gebel El-Galala El-Bahariya and Gebel Ataqa. The main trend of tectonic joint in the zone of these faults revels also the general northeast-southwest, north-south and northwest-south-southeast directions.

2.4. Subsurface stratigraphy

The subsurface stratigraphy in the study area has been described through Water well which drilled by geological survey of Egypt, 1999 (Fig. 2). The Water well description indicates that the Quaternary deposits represented by wadi deposits, sand and gravel of thickness about 4 m. These Quaternary deposits overlay Upper Miocene deposits which represented by calcareous sandstone and argillaceous sandstone deposits and have thickness of 45 m. Middle Miocene is represented by thin layer of clay, sandstone deposits and limestone at the base of Water well. This sandstone is saturated by fresh water and has thickness of 40 m.

3. Methodology

3.1. Geoelectrical measurements

The electrical investigation area extends 6.89 km in width by 3.67 km in length. A total number of 27 Schlumberger Vertical Electrical Soundings (VES) were conducted in the study area with maximum current electrode half-spacing (AB/2) of 1000 m. All

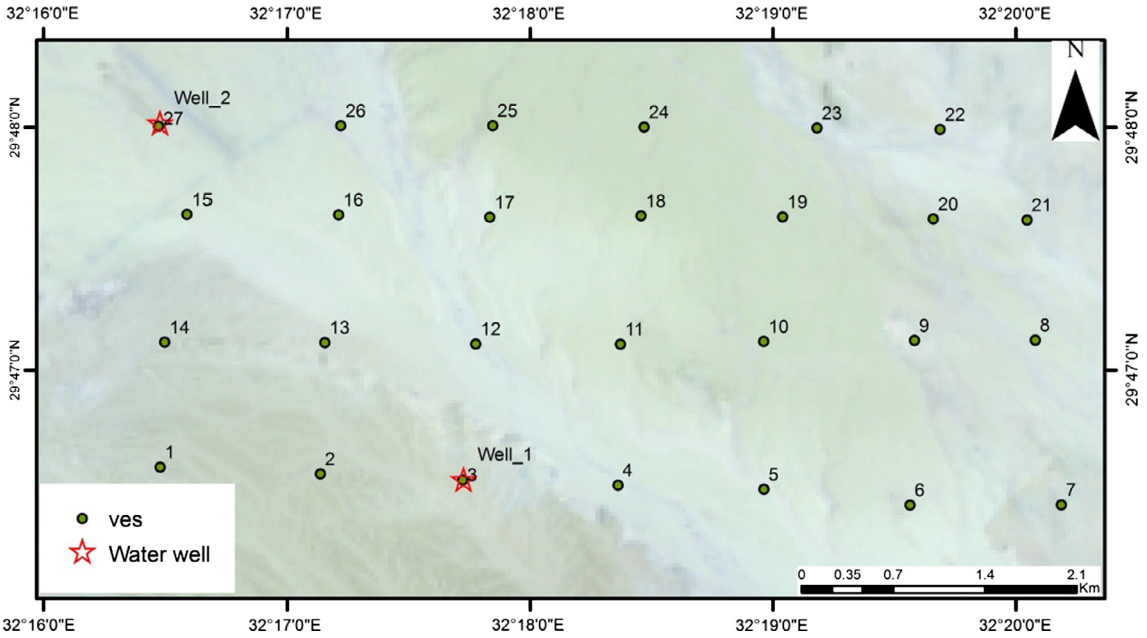

Fig. 3. Location map for the conducted vertical electrical sounding (VES) at the study area.

VES were well distributed taking into consideration the complex tectonic system of the study area. Some VES were conducted very close to available water wells to correlate the well data with the resultant resistivity data (Fig. 3). Resistivity measurements were carried out using SYSCAL_R2 (IRIS, France). The specification of instrument can be described. A DC current was injected into the earth via two current electrodes and the potential difference between the two electrodes was measured via two potential electrodes. Apparent resistivity was then calculated by multiplying the geometric factor of the used Schlumberger array by the measured resistance value. The resistivity data was measured every sixth of a logarithmic decade to ensure interpretation accuracy (Loke, 1999).

3.2. Interpretation of resistivity sounding curves

Electrical resistivity soundings data could be interpreted quantitatively and qualitatively.

3.3. Quantitative interpretation methods

The aim of the quantitative interpretation of the vertical electrical soundings is to determine the thickness and true resistivity values of the successive strata below the different stations, utilizing the measured field data, which are represented by plotted the apparent resistivity values against AB/2 spacing. This plotted data are called the vertical electrical curves. There are several methods for the quantitative interpretation of the electrical data. Some of them are graphical method is carried out using the two layers curve and the generalized Cagniard graphs (Kooefoed, 1960) to convert the values of (AB/2) and apparent resistivity values (ρa) into a number of layers model of thicknesses and true resistivity.

Another technique of quantitative interpretation is the analytical method (computer program), which is defined as IPI2WIN program. The obtained results of the manual interpretation were used as initial models for the analytical methods. The IPI2WIN program has been designed by a scientific group in Moscow state university, Russian at 2000. This program deals with VES curves in man-computer interactive regime and draws theoretical and field curves on a display screen together with Rho (Z) model curve. The quantitative interpretation has been applied to determine the thickness and true resistivities of the stratigraphic units below each VES stations. Two VES statins no. (3 and 27) (fig. 3) were located at Water well no. (1 and 2) successively which drilled by geological survey of Egypt (EGSMA, 1999) to correlated and calibrate the VES curves parameters (layer resistivity and thickness). Fig. 4 represents examples for the interpretation for some VES stations using IPI2-WIN PROGRAM.

3.4. Data analysis and interpretation

The interpreted VES stations were used to produce six geoelectric cross sections (fig. 5). Data from oil, exploration and/or water wells were integrated in these sections. Faults shown in these cross-sections were confirmed from geological subsurface studies performed in the study area and magnetic interpretation. A total of 6 subsurface layers were recognized in the geoelectric cross sections from top to bottom as follows:

1. The first geoelectric unit that exhibited in all VES stations is characterized by very high to high resistivity values ranged between 113 Ω·m and 11,291 Ω·m, which correspond to surface gravel and sand (wadi deposits) of Quaternary deposits. The thickness of this unit is ranged between 2.44 m and 5.4 m. Variations in the resistivity values of this layer could be attributed to two main reasons: areal variations in the grain size distribution and variation in the gravel-sand-silt-clay ratios. The thickness of this layer ranges between 0.508 m and 5.41 m.
2. The second geoelectric unit is exhibited in all VES stations; it exhibits resistivity values ranging from 37.68 Ω·m to 343 Ω·m, which corresponds to calcareous sandstone. The thickness of this unit is varied from 2 m to 24.5 m.
3. The third geoelectric unit is characterized by very moderate to low resistivity values varied from 2.5 Ω·m to 34.4 Ω·m, which corresponds to argillaceous sandstone of middle Miocene. The thickness of this unit is varied from 5 to 44.8 m.
4. The fourth geoelectric unit is manifested by moderate to high resistivity values varied from 25.5 Ω·m to 200 Ω·m, which correspond sand and sandstone. The thickness of this unit is varied from 12 m to 45 m.

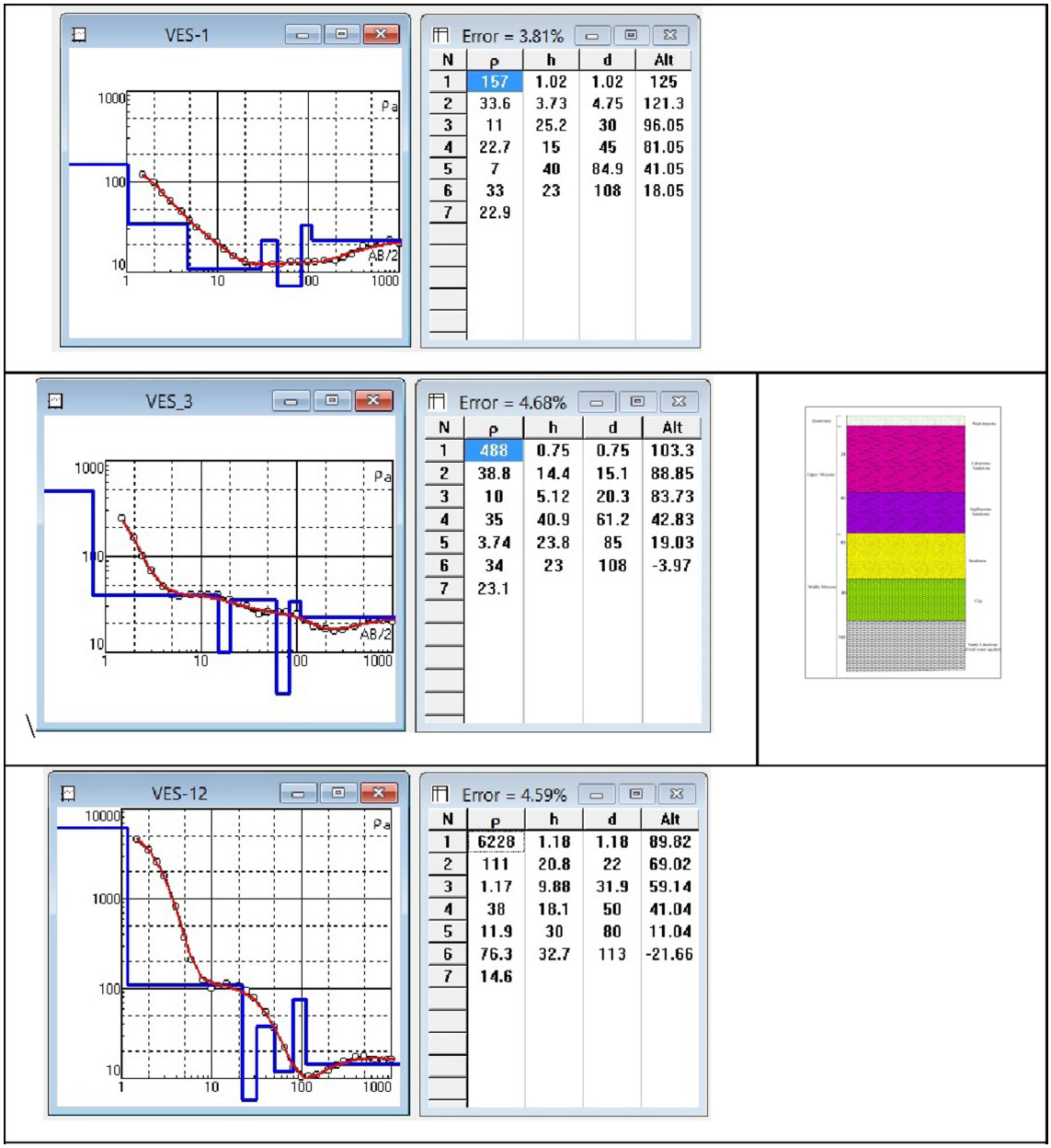

Fig. 4. Correlation between the interpreted resistivity layers of the selected VES's and the given water well data (using IPI2win program).

5. The fifth geoelectric exhibits resistivity values ranging from 5 Ω·m to 45 Ω·m which corresponds to sandstone intercalated with clay (clayey sand) of Middle Miocene deposits. The thickness of this unit is varied from 14 m to 43.
6. The sixth geoelectric unit is implicated by moderate to high resistivity values ranged between 10 Ω·m and 88 Ω·m, which corresponds to calcareous sandstone and limestone with fresh groundwater of Middle Miocene deposits. The lower surface of this unit is not detected at any VES.

This unit is the Middle Miocene aquifer correlated with the some corresponding adjacent water table (obtained from the existing Water well) which consists of sandstone and as the water bearing unit. This unit has resistivity values ranging from 17 Ω·m to 87 Ω·m. The map Fig. 6 shows that the true resistivity values increase around VES 2, 12,10,5, 22, 23 and 24. The depth map for the top surface of the aquifer (Fig. 7) indicates that the northern and north eastern parts of the study area reflects deep depths about 97–110 m, but the south western parts reveal shallow depths of 70–77 m

4. Hydrological budget of the basins in the study area

Hydrographic parameters associated with the drainage basins of the study area are given in Table 1. However, the infiltration capabilities and groundwater potentiality for the rocks of the study area are given in Table 2.

5. Site selection model

A site selection model is a decision making tool for identifying locations in a landscape where multiple criteria overlap in geographic space (Wilson, 2008). The primary goal of this study is development a methodology to locate suitable locations for constructing dams and the secondary goal is to identify the factors which govern this selection. GIS program was used as a tool helps to attain this goal.

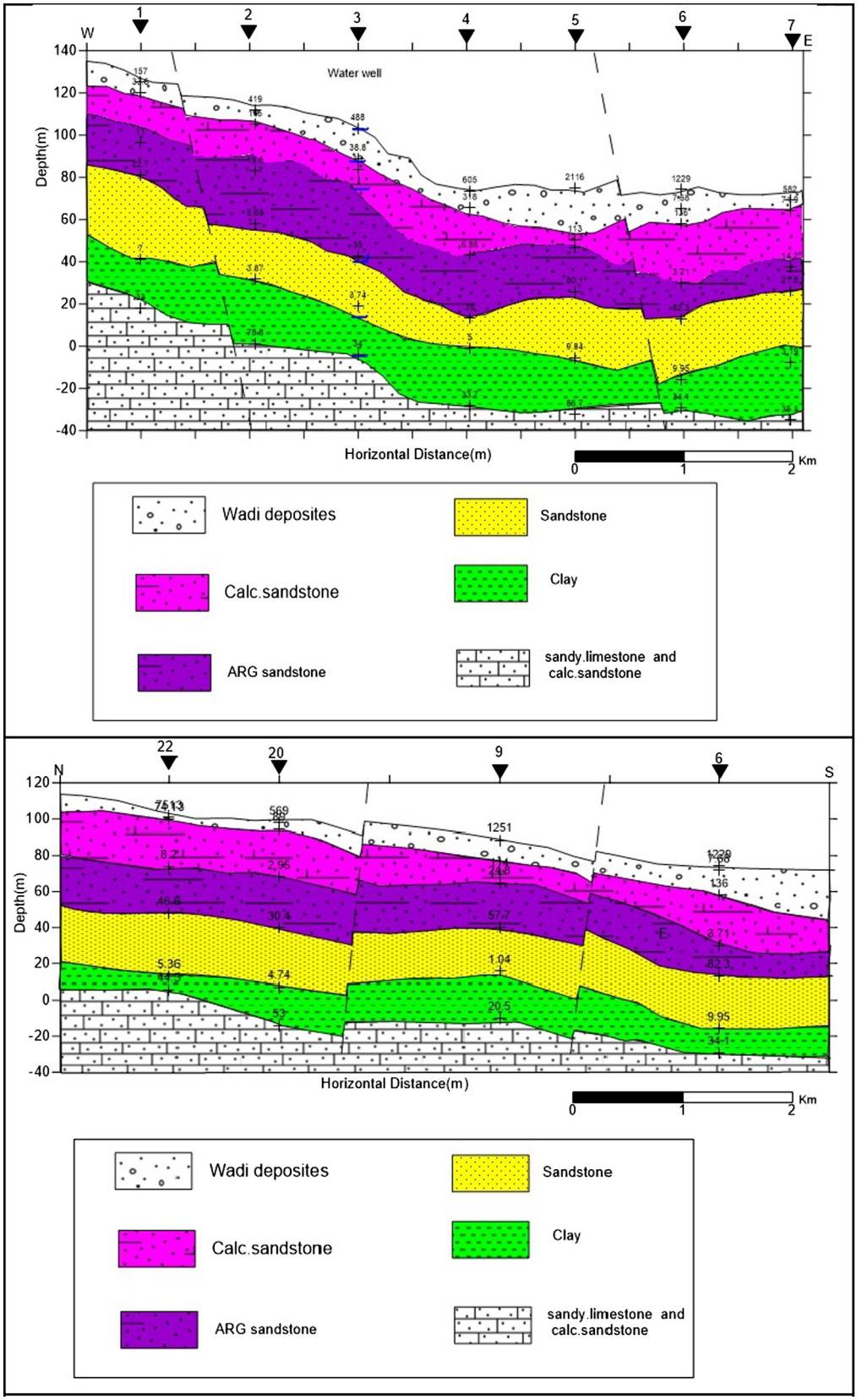

Fig. 5. The geoelectric cross-sections in the study area.

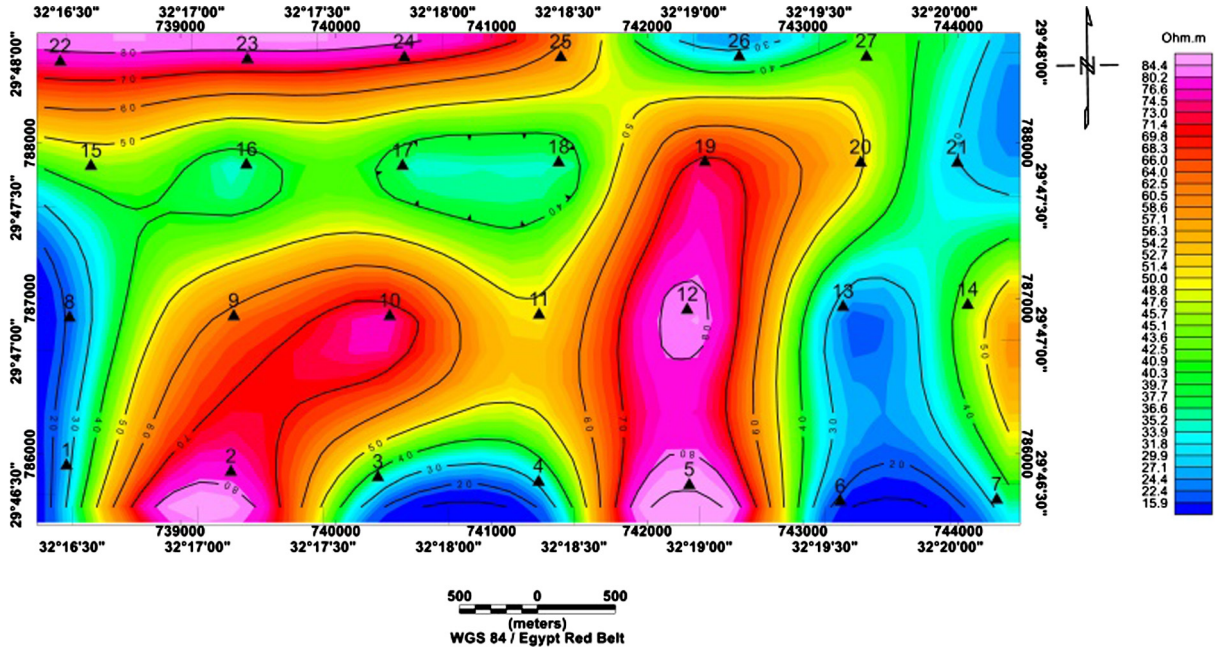

Fig. 6. True resistivity map for the sixth geoelectric unit.

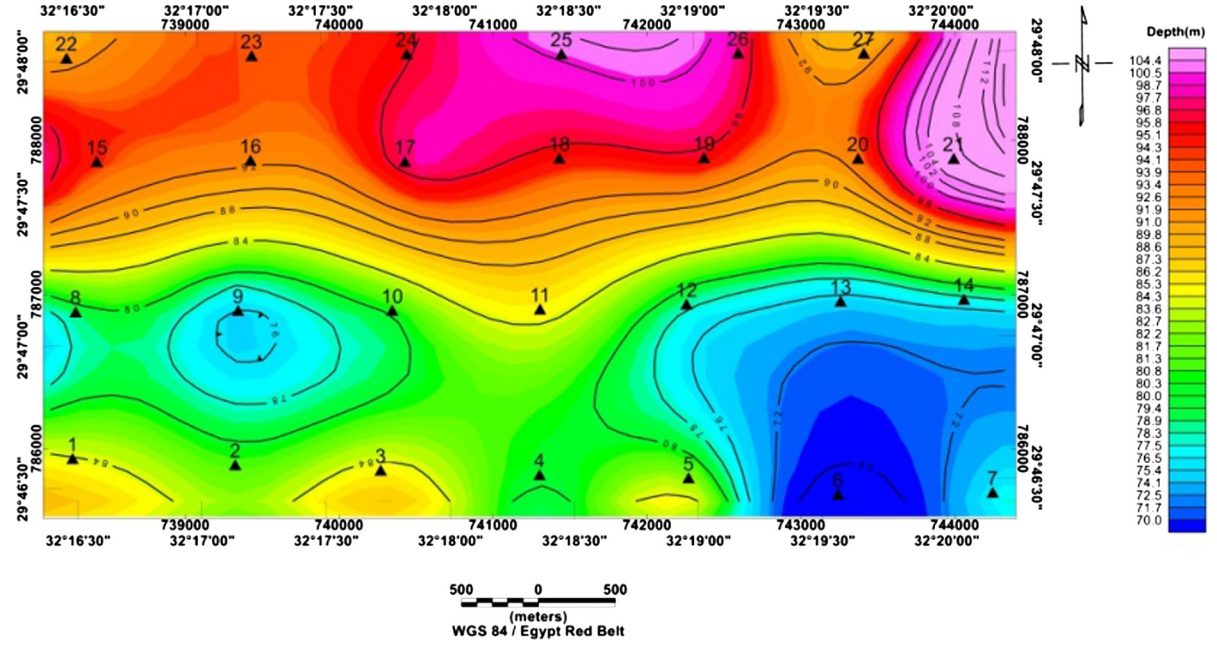

Fig. 7. Depth map of the upper surface for aquifer.

Table 1
Hydrographic parameters and WMS outputs for the study area drainage basins.

Wadi (valley) name	Area (km^2)	Total runoff (m^3/year)	Surface runoff (m^3/year)	Net groundwater recharge (m^3/year)	Time to peak discharge (min)
Hammath	115.7	891,107	317,032	479,292	1501
Hugal	383.119	3,007,619	1,079,173	1,589,808	1455

Table 2
Major exposed rocks in the study area according to their infiltration capabilities and groundwater potentiality.

Major lithologic groups	Soil hydrologic group	Infiltration rate (mm/h)	Groundwater potentiality
Wadi deposits, sand and gravel sandstone	A	High infiltration >6.09	High

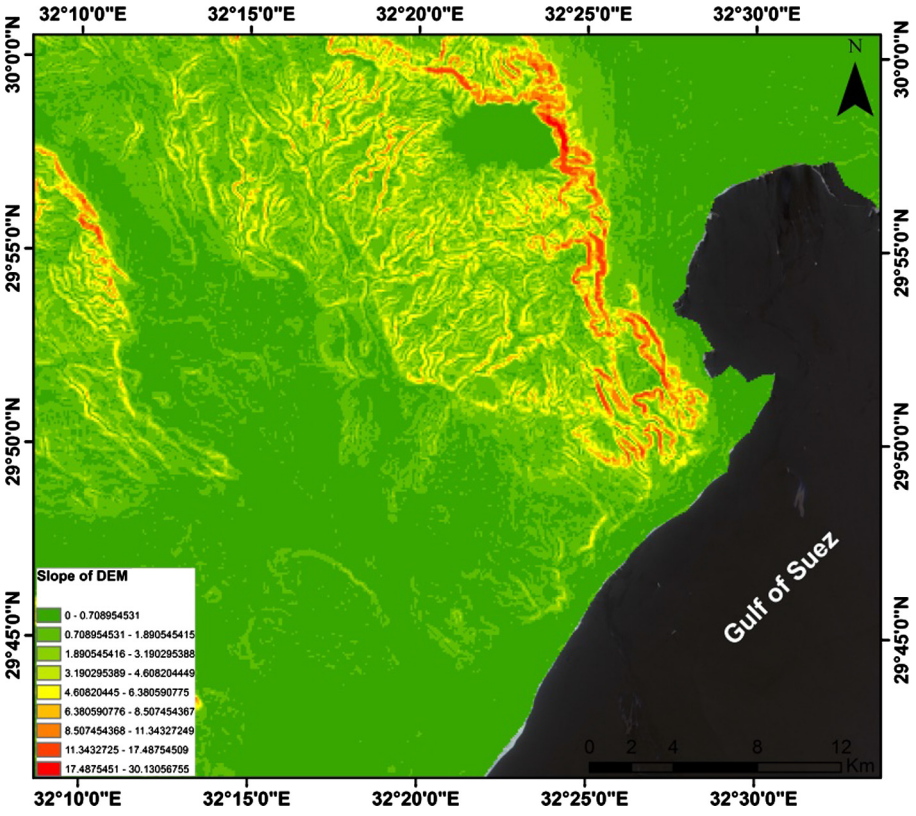

Fig. 8. Slope for DEM of the study area.

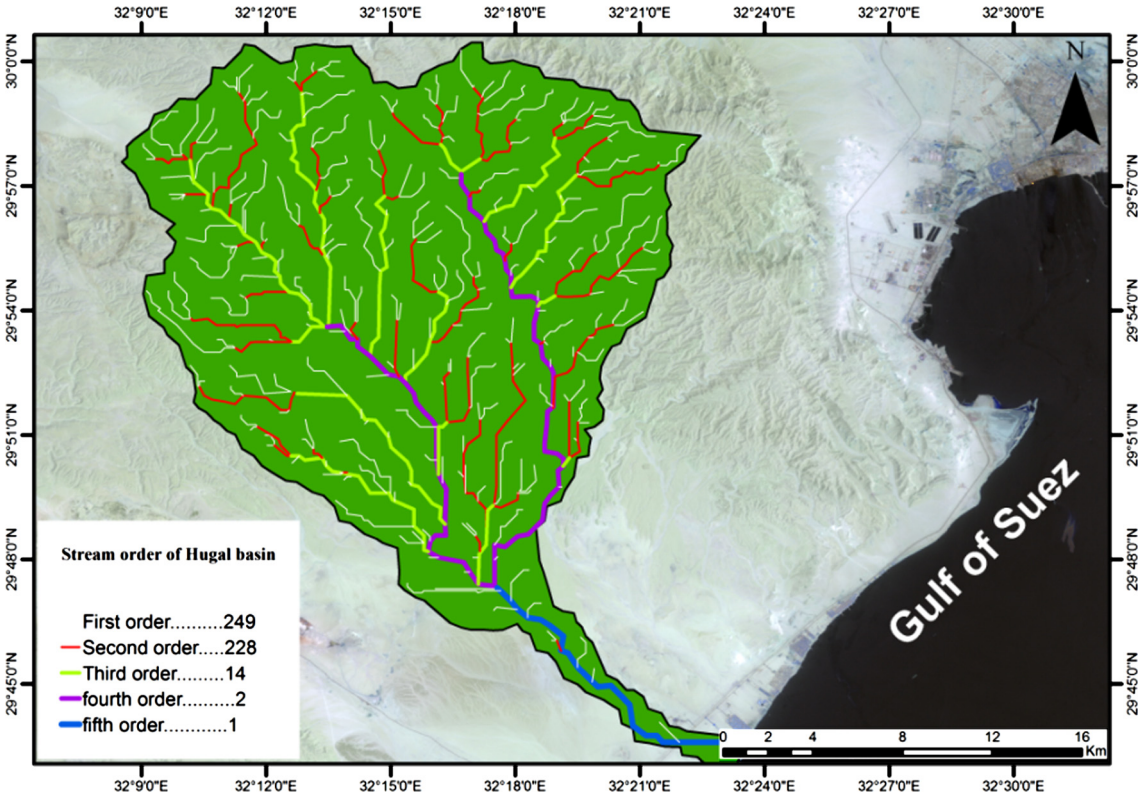

Fig. 9. Stream order of Hugal basin.

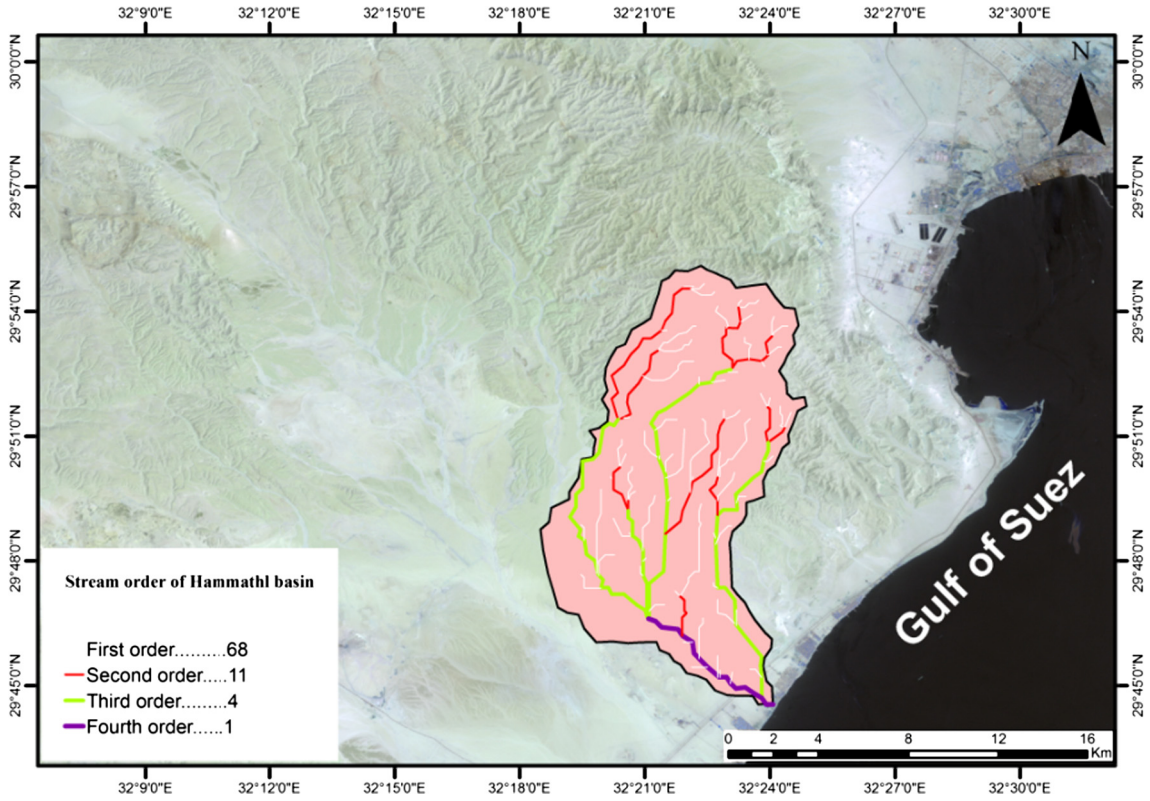

Fig. 10. Stream order of Hammath basin.

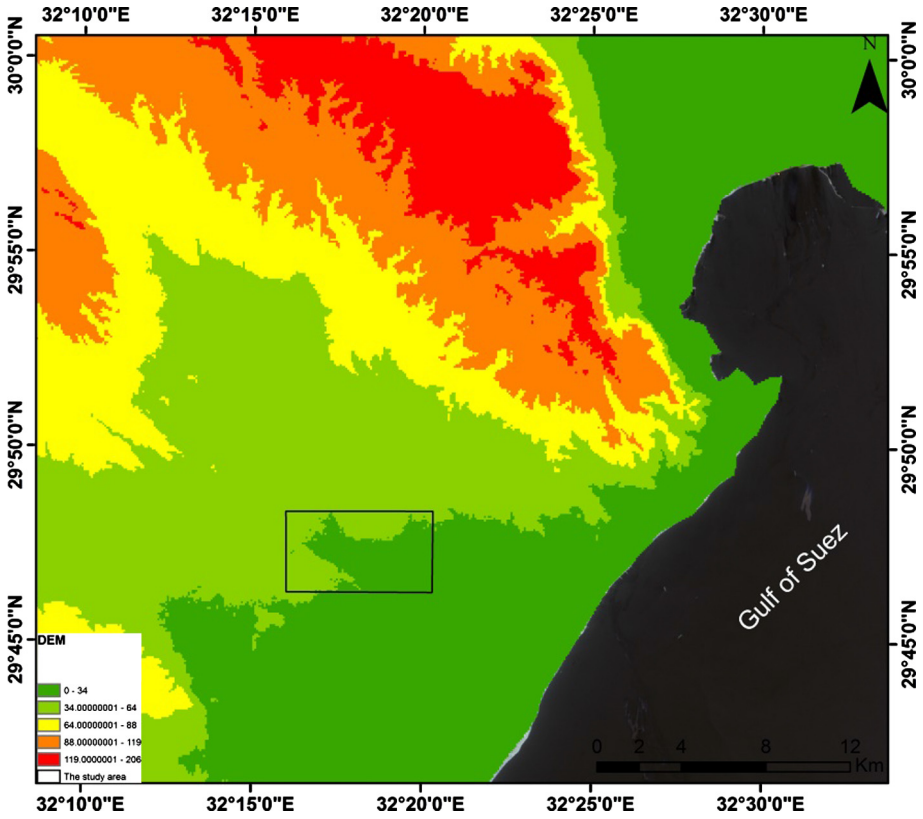

Fig. 11. Digital Elevation Model (DEM) of the study area.

5.1. Conditions that govern the selection of the suitable locations for dams' construction

- **Slope:**

Slopes help to identify the maximum rate of change in surface value over a specific distance and they are expressed in degrees or percentage (Ziadat et al., 2006). The slope map (Fig. 8), was obtained from the DEM shows the slope variation in the study area.

- **Earthquakes:**

Seismic activity is the study of the distribution of earthquakes and their characteristics within a particular region. The most important aspects of seismic activity are given by the geographic distribution of earthquakes' foci, their magnitude and their occurrence over time. The mechanisms and the damage produced by the earthquakes that affected this area, were studied by Dahy (2010). It is important to build dams on the site with low seismicity to protect the downstream life and property. Generally, strong ground shaking can result instability of the dam and strength loss of foundations (Seed et al., 1969; Seed et al., 1975; Jansen, 1988; Castro et al., 1985).

- **Buildings and roads:**

In general, buildings couldn't to be located near dams because their sewage pipelines can affect the soil cohesion where dams are built. Also dams have to be away from roads where traffic can cause vibrations in dams' bodies like earthquakes.

- **Drainage network:**

The dams are preferred to be built on the main stream order where the most common point of collection of rainfall (Figs. 9 and 10).

Table 3
The layer using in model.

Criteria	Data	Source	Scale	Type
1	Drainage network	STRM 2008 (Figs. 9 and 10)	Line	Pixel resolution 30 m
2	Elevation/topography	STRM 2008 (Fig. 11)	Grid	Pixel resolution 30 m
3	Slope	STRM 2008 (Fig. 8)	Grid	Pixel resolution 30 m
4	Buildings	Quikbird (2008)	Point	Pixel resolution 60 cm
5	Roads	Quikbird (2008)	Line	Pixel resolution 60 cm
6	Earthquakes	Data of the National Institute for Astronomical and Geophysical studies (Helwan observatory) (from 1900 to 2004)	Point	–
7	Faults	The Egyptian geological survey map 2001	Line	1:250,000

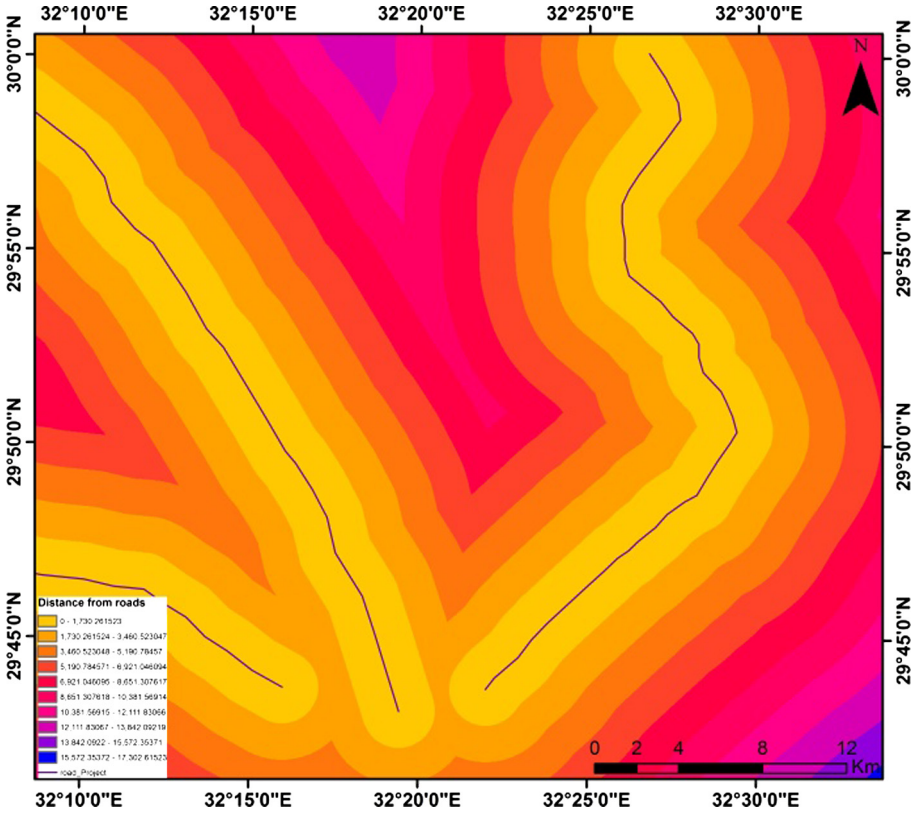

Fig. 12. Distance from the road in the study area.

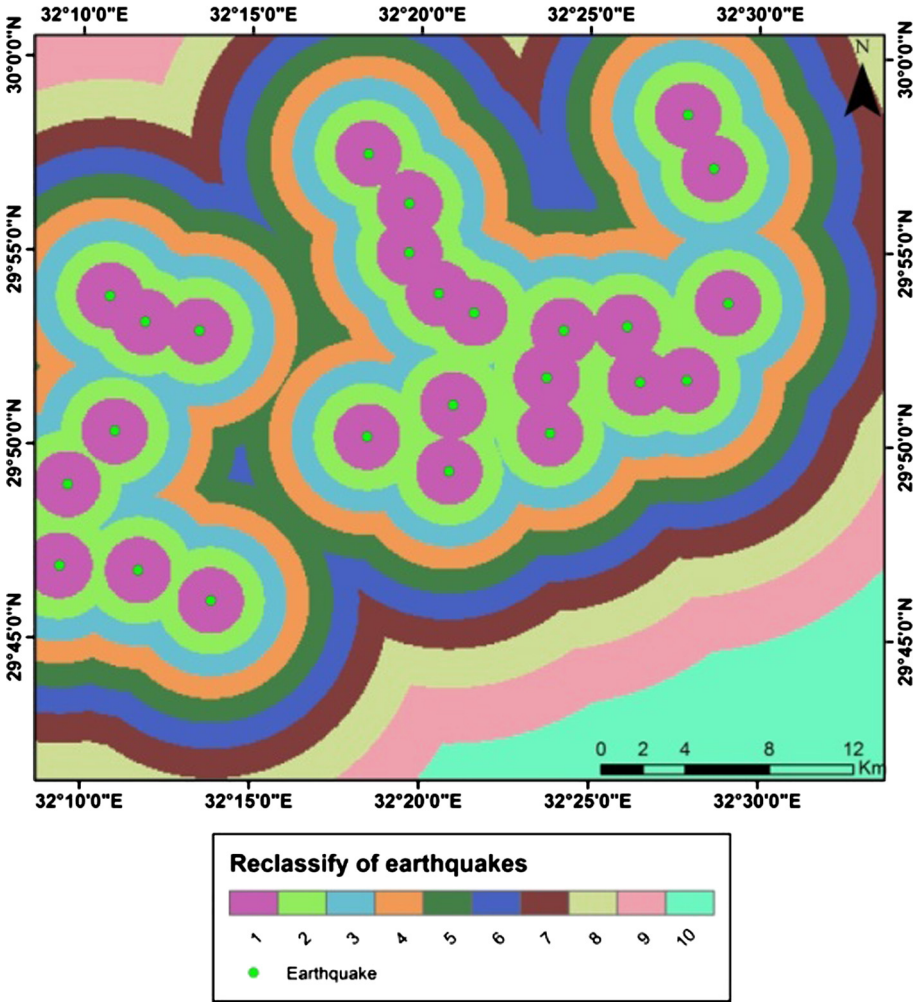

Fig. 13. Reclassify for earthquakes in the study area.

5.2. The layers using in model

Drainage Network, Elevation, Slope, Buildings, Roads, Earthquakes and Faults were used as input data in model which were explained in Table 3. They governed the selection of the suitable locations for dams' construction. They were explained in detail in paragraph 1.

5.3. Methodology

It will be built a suitability model with ArcGIS Spatial Analyst extension tools that finds suitable locations for a dam's construction. The steps to produce such a suitability model are outlined below:

(1) Drainage Network, Elevation, Slope, Buildings, Roads, Earthquakes and Faults were used to design site selection model in Table 3 as input for model;
(2) Deriving distance from recreation sites; Euclidean distances were estimated to calculate the distance between every layer and surrounding grids. In other word, it must first be calculated the Euclidean (straight-line) distance from recreation sites. On the Distance to recreation sites layer, distances increase the farther you are from a recreation site (ESRI, 2011).one sample of maps was shown in Fig. 12.
(3) Reclassifying datasets: Deriving datasets, such as slope, is the first step when building a suitability model. Each cell in the study area now has a value for each input criteria (distance to Drainage Network, distance to Elevation, distance to Buildings, distance to Roads, distance to Earthquakes, distance to Faults, Slope). It needs to be combined the derived datasets so it can be created the suitability map that will identify the potential locations for the dams' construction. However, it is not possible to combine them in their present form so the next step was to reclassify the previous maps where they were classified into a relative friction of 10 classes in order to have a common value. In the classified maps, the number "10" indicated good areas to construct dams while the number "1" indicated bad areas. For example, it is necessary to construct dams away from earthquakes to protect the downstream life and property so It will be reclassified the Distance to earthquakes layer, assigning a value of 10 to areas farthest from existing earthquakes (the most suitable locations), assigning a value of 1 to areas near earthquakes (the least suitable locations), and ranking the values in between linearly. By doing this, it will be determined which areas are near and which areas are far from earthquakes. One sample of maps was shown in Fig. 13.
(4) Weighting and combining datasets.

It is now ready to combine the reclassified datasets to find the most suitable dams construction. The values of the reclassified datasets have all been reclassified to a common measurement scale (more suitable cells have higher values) and weighted each accord-

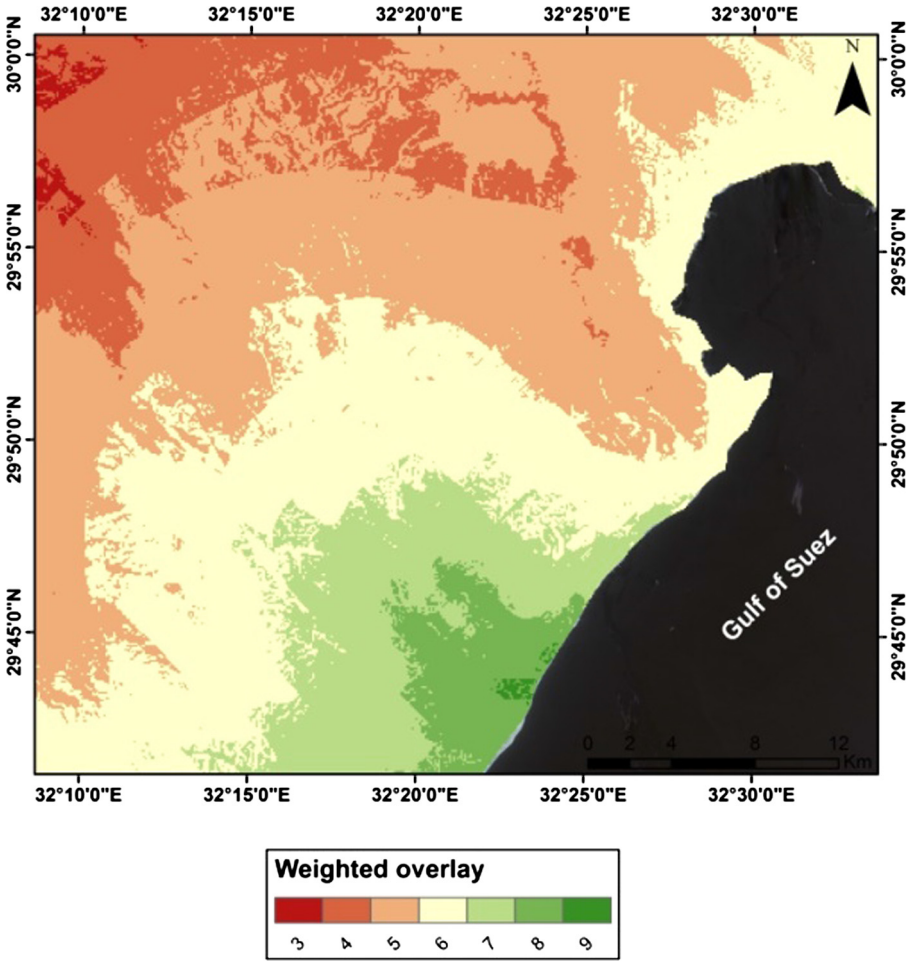

Fig. 14. Weighted overlay of the used layers

Table 4
Weighted overlay model.

Number	Layer name	Rank	Weight = (rank − layer No.) + 1	Normalized weight = weight/sum * 100
1	Earthquakes	4	3	9
2	Hugal drainage network	1	6	20
3	Hammath drainage network	1	6	20
4	Faults	4	3	9
5	Buildings	5	2	6
6	Road	5	2	6
7	DEM	2	5	17
8	Slope	3	4	13
Sum				100%

Table 5
Intensity of importance.

Intensity of importance	Definition
1	Very to extremely strong importance
2	Very strong importance
3	Strong to very strong importance
4	Strong importance
5	Moderate to strong importance

ing to its importance where it will be weighted all the inputs, assigning each a percentage of influence (Fig. 14). The higher the percentage, the more influence a particular input will have in the suitability model (Tables 4 and 5).

(5) Selecting optimal sites

Now each pixel has a value that indicates how suitable that location is for dams' construction. Pixels with the value of 10 are most suitable, and pixels with the value of 0 are not suitable. Therefore, the optimal site location for dam construction has the value of 10. Another criteria for an optimal location is the size of the suitable area. A suitable location would include several pixels with value of 10 being connected. It will be used a conditional expression in the Con tool to extract only the optimal sites. It has been decided that those sites that are considered optimal must have a suitability value of 10 (the highest value in the suit areas output). In the conditional expression, all areas with a value of 10 will retain their original value (10). Areas with a value of less

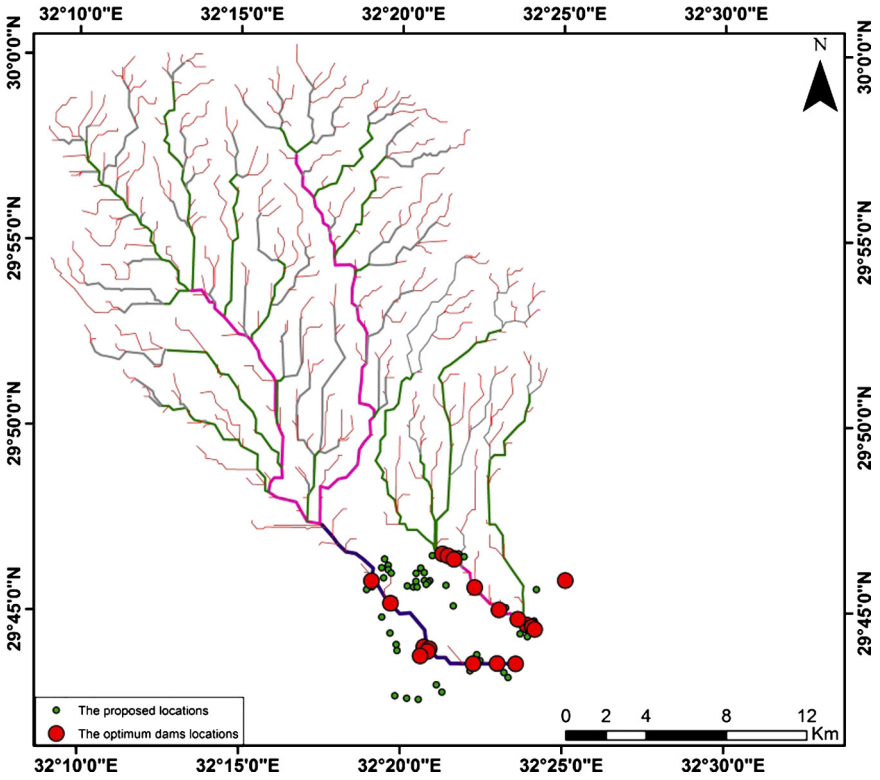

Fig. 15. Drainage system in the study area, the blue points show the proposed locations from model and the red points show the optimum locations of dams by interpreter.

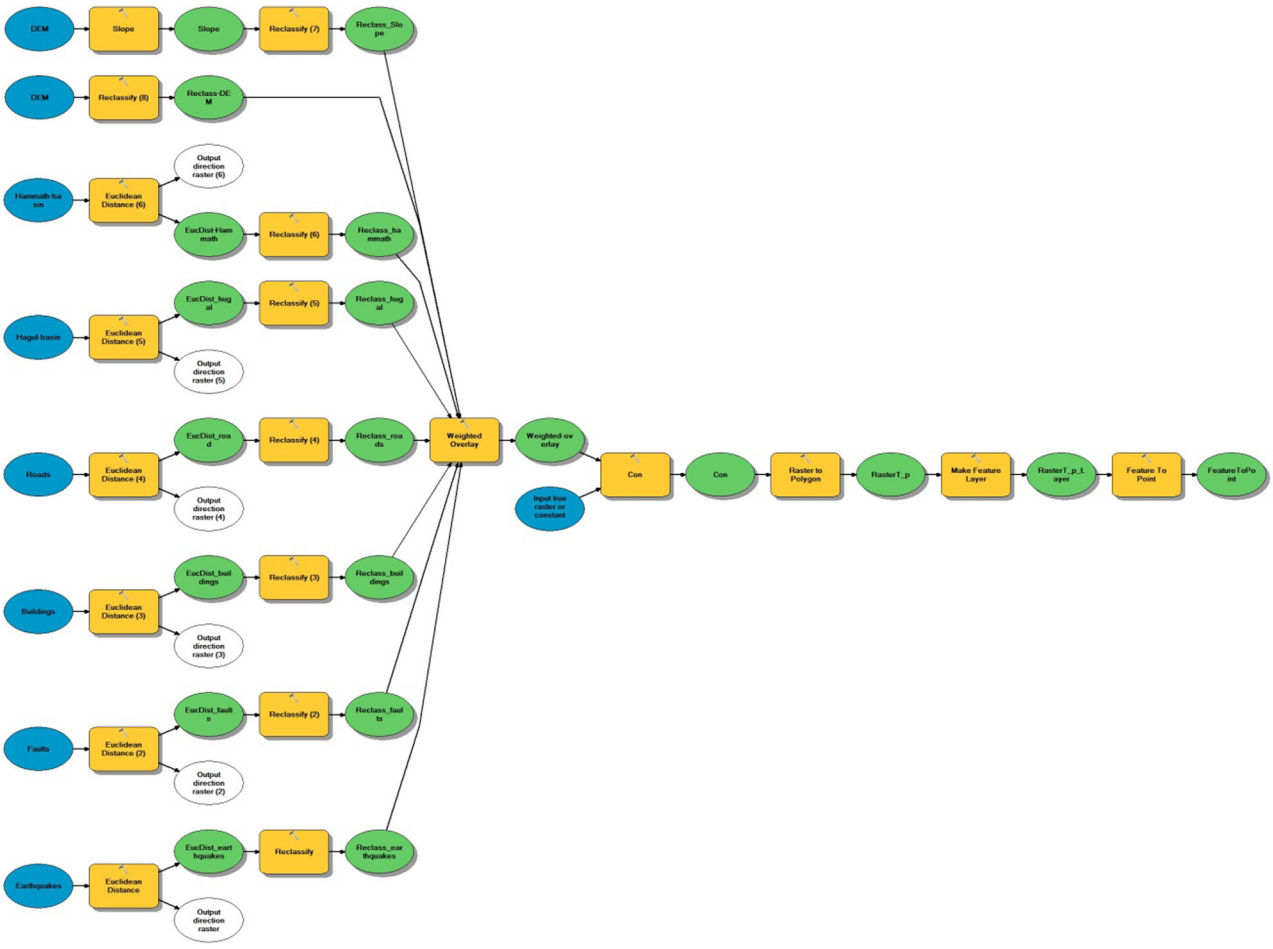

Fig. 16. Flow chart of site selection model.

than 10 will be changed to No Data (ESRI, 2011) (Fig. 14). Then applying feature to points tool which creates a feature class containing points generated from the representative locations of input features (ESRI, 2011). Where the tool proposes several locations while the interpreter tries to find the optimum locations for construction dams where the highest amount of water (Fig. 15). Flow chart showing the procedures to establish the site selection model for selecting the suitable locations for construction dams (Fig. 16).

6. Conclusions

According to the results of the interpretation of the geoelectrical parameters, hydrological data and geographic information systems (GIS), was a successful approach in the site selection process to identify the optimum locations for dam construction. The results of the Vertical Electrical Sounding (VES) showed that the fresh aquifer is the unit is the lower Miocene aquifer which consists of sandstone and as the water bearing unit. This unit has resistivity values ranging from 17 Ω·m to 87 Ω·m. The depth for the top surface of the aquifer Indicates that the northern and north eastern parts of the study area reflects deep depths about 97–110 m, but the south western parts reveal shallow depths of 70–77 m. It could be concluded that the combination of geophysical analysis and fieldwork along with remote sensing and GIS is a successful and cost-effective approach in the assessment of groundwater in north western Gulf of Suez.

Acknowledgments

The authors would like to express them sincere thanks and deep appreciation to the staff of the Geophysical Department, Cairo University and the staff of National Authority for Remote Sensing and Space Sciences, Cairo, Egypt and the staff of National Research Institute of Astronomy and Geophysics, Helwan, Cairo.

References

Abd El Nasr, R., 1979. The geology of Hammtih and Wadi Gamal at north of Gulf of Suez. Faculty of Science, Ain Shams University, Cairo.
Abd El Rahman, H., 2001. Evaluation of groundwater resources in Lower Cretaceous aquifer system in Sinai. Water Resour. Manage 15 (3), 187–202.
Abdallah, A.M., Alindani, E.A., 1993. Stratigraphy of upper Paleozoic rock western side of the Gulf of Suez. Minist. Geol. Surv. 18.
Abdallah, M.A., Abd El-Hady, F.M., 1966. Geology of Sadat area, Gulf of Suez. J. Geol. UAR 10, 1–24.
Abd-Elshafy, E., Abed, M.M., Shahat, W., 1989. Stratigraphic correlation and macropaleontology of Akheider-Um Zeita Eocene successions. In: Gulf of Suez Egypt – Proc. Symp. Phanerozoic & Development in Egypt. National Committee of Geological Sciences & Al-Azhar University, pp. 79–106.
Abu El-Anwar, E.A., El-Gohary, A.M., 2003. Petrographical and geochemical characteristics of Sadat formation and its depositional environment, Sadat Area, West Gulf of Suez, Egypt. J. Sediment. Res. 11, 77–94.
Abu El-Enain, F.M., Ali, M.M., Ismail, A.S., 1995. Petrography, geochemistry and depositional history of the Eocene rocks in the area between northern Galala and Gabal Ataqa, Western Gulf of Suez, Egypt. Ann. Geol. Surv. Egypt XX, 551–576.
Al Ahwani, M.M., 1982. Geological and sedimentological studies of Gebel Shabraweet area, Suez Canal District, Egypt. Ann. Geol. Surv. Egypt, 305–381.
Bignot, G., Strougo, A., 2002. Middle Eocene benthic foraminiferal assemblages from eastern Egypt, as biochronological and peritethyan lagoonal indicators. Rev. Micropaleontol., 73–98
Butzer, K.W., 1960. Environmental and Human Ecology in Egypt during Pre-Dynastic and Early Dynastic Times, Vol. 33. Bulletin de la Societé de Géographie d'Egypte, France.
Castro, G., Poulos, S.J., Leathers, F., 1985. Re-examination of Slide of Lower San Fernando Dam. J. Geotech. Eng. 111 (9), 1093–1107.
Cuvillier, J., 1941. L Eocene de la region de suez et ses rapports avec le Gretace superieur. Bull. Soc. Geol. Fr., 25–34
Dahy, S.A., 2010. A study on seismicity and tectonic setting in the northeastern part of Egypt. Res. J. Earth Sci. 2 (1), 8–13.
EGSMA, 1999. Geotechnical study and groundwater exploration for the free economic area, northwest Gulf of Suez, Egypt (internal report).
El Attar, A.A., 2003. Early middle Miocene echinoids from Sadat formation Sadat area, South Gebel Ataqa NW, Gulf of Suez, Egypt. J. Paleontol., 209–241
ESRI, 2011. Watershed Delineator Application User's Manual. Environmental Systems Research Institute, Redlands, CA.
Ettinger, M., Langozki, Y., 1969. Hydrodynamics of the Mesozoic Formations in the Northern Negev, Vol. 46. State of Israel Ministry of Development, Jerusalem.
Hassan, S.M., 2008. Studying of geological structures of Ayn-Sokhna area, north Eastern Desert Egypt, by optimum utilization of data fusion techniques of some satellite image Ph.D. Thesis. Faculty of science, Helwan University, p. 207.
Jansen, R.B., 1988. Advanced Dam Engineering for Design. Construction and Rehabilitation. Van Noswtrand Reinhold. 884.
Khalil, M.H., 2006. Geoelectric resistivity sounding for delineating salt water intrusion in the Abu Zenima Area, West Sinai, Egypt. J. Geophys. Eng., 243–251
Kooefoed, O., 1960. A generalized Cagniard graph for interpretation of geoelectric sounding data. Geophys. Propect. 8, 459–469.
Loke, M.H., 1999. Electrical imaging surveys for environmental and engineering studies. Egypt.
Masoud, A., Koike, K., 2005. Remote sensing and GIS integration for groundwater potential mapping in Sinai Peninsula, Egypt. Proceedings of International Association for Mathematical Geology (IAMG'05): GIS and Spatial Analysis, Toronto, 1, pp. 440–445.
Mills, A.C., Shata, A., 2009. Ground-water assessment of Sinai, Egypt. Groundwater 27, 793–801.
Moustafa, A.R., Abdallah, A.A., 1991. Structural Setting of the Central Part of the Cairo-Suez District. Ain Shams University, pp. 133–145.
Norconsult, A.S., 1979. Structure plane for Suez Governorate. Groundw. Resour. Investig. 64.
Renolds, M.L., 1979. Geology of the Northern Gulf of Suez. Ann. Geol. Surv., 322–343
Sadek, H., 1926. The geography and geology of the district between Gebel Ataqa and El Bahariya (Gulf of Suez). Egypt. Geol. Surv., 120
Salem, A.S., 1988. Geological and hydrogeoloical studies in the area between Gebel Ataqa and Northern Galala. Faculty of Science, Zagazig University, Egypt.
Seed, H.B., Lee, K.L., Idriss, I.M., 1969. Analysis of Sheffield Dam failure. J. Soil Mech. Found. Div. 95, 1453–1490.
Seed, H.B., Lee, K.L., Idriss, I.M., Makdisi, F.I., 1975. The slides in the San Fernando Dams during the Earthquake of February 9, 1971. J. Geotech. Eng. 101, 651–688.
Strougo, A., 1985a. Eocene stratigraphy of the eastern Greater Cairo (Gebel Mokattam-Helwan) area. Middle East Res. Centre, Ain Shams Univ., Sci. Res. Ser., 1–39
Strougo, A., 1985b. Eocene stratigraphy of the Giza Pyramids Plateau. Middle East Res. Centre, Ain Shams Univ., Sci. Res. Ser., 79–99
Strougo, A., Abdallah, A.M., 1990. Mokattamian stratigraphy of north central Eastern Desert (South of Maadi-Qattamiya road). Faculty of Science, Ain Shams University.
Strougo, A., Boukhary, M., 1987. The Middle Eocene – Upper Eocene boundary in Egypt. Revue de Micropaléontologie 30, 122–127.
Sultan, A.S., Hewaidy, A.G., El-Motaal, E.A., Ramdan, T.M., El khafif, A.A., Soliman, S. A., 2015. Groundwater exploration using resistivity and magnetic data at the northwestern part of the Gulf of Suez, Egypt. Egypt. J. Petrol. 9.
Sultan, S.A., Mohamed, B.S., 2000. Geophysical investigation for groundwater at Wadi Ghuwaybah, Northern Part of Eastern Desert, Egypt. Annals of Geological Survey of Egypt XXIII, 901–918.
Teufik, N., 1988. An exploration outlook on the Northern Gulf of Suez, Egypt. Earth Resour. Explor. (EREX) 26.
Wilson, J., 2008. Retrieved from <www.iupui.edu: http://www.iupui.edu/~geospace/kibi_web/model.html>.
Youssef, M.I., Abd Rahman, M.A., 1978. Structural map by remote sensing of the area between Gebal Ataqa and the Northern Galala Plateau Gulf of Suez Region, Egypt. In: Tenth Arab Petroleum Conference Tripoli, Libya, 135(1–3), p. 8.
Youssef, M.S., EL Hakim, H., Awad, W.K., Shaban, M.M., Nimnim, M.E., 1966. Geophysical Investigations for Groundwater in EL-Maghara Area, Northern Sinai. Egyptian Geological Survey, Cairo, p. 42.
Ziadat, F.M., Mazahreb, S., Oweis, T.Y., Bruggeman, A., 2006. A GIS-based approach for assessing water harvesting suitability in a Badia benchmark watershed in Jordan. In: Soil Conservation Organization (ISCO) Conference, Marrakech, Morocco.